Virology 484 (2015) 313–322

Contents lists available at ScienceDirect

Virology

journal homepage: www.elsevier.com/locate/yviro

Brief Communication

A G-quadruplex-binding macrodomain within the "SARS-unique domain" is essential for the activity of the SARS-coronavirus replication–transcription complex

Yuri Kusov [a,b], Jinzhi Tan [a], Enrique Alvarez [1,c], Luis Enjuanes [c], Rolf Hilgenfeld [a,b,*]

[a] Institute of Biochemistry, Center for Structural and Cell Biology in Medicine, University of Lübeck, Lübeck, Germany
[b] German Center for Infection Research (DZIF), Hamburg – Lübeck – Borstel Site, University of Lübeck, Germany
[c] Department of Molecular and Cell Biology, Centro Nacional de Biotecnología (CNB-CSIC), Campus Universidad Autónoma, Madrid, Spain

ARTICLE INFO

Article history:
Received 1 March 2015
Returned to author for revisions
19 March 2015
Accepted 12 June 2015

Keywords:
SARS-CoV replicon
SARS-unique domain
Macrodomain
X-domain
Reverse genetics
G-quadruplex
MERS-CoV

ABSTRACT

The multi-domain non-structural protein 3 of SARS-coronavirus is a component of the viral replication/transcription complex (RTC). Among other domains, it contains three sequentially arranged macrodomains: the X domain and subdomains SUD-N as well as SUD-M within the "SARS-unique domain". The X domain was proposed to be an ADP-ribose-1"-phosphatase or a poly(ADP-ribose)-binding protein, whereas SUD-NM binds oligo(G)-nucleotides capable of forming G-quadruplexes. Here, we describe the application of a reverse genetic approach to assess the importance of these macrodomains for the activity of the SARS-CoV RTC. To this end, Renilla luciferase-encoding SARS-CoV replicons with selectively deleted macrodomains were constructed and their ability to modulate the RTC activity was examined. While the SUD-N and the X domains were found to be dispensable, the SUD-M domain was crucial for viral genome replication/transcription. Moreover, alanine replacement of charged amino-acid residues of the SUD-M domain, which are likely involved in G-quadruplex-binding, caused abrogation of RTC activity.

Introduction

The Severe Acute Respiratory Syndrome coronavirus (SARS-CoV) belongs to lineage b of the genus *Betacoronavirus*. During the SARS outbreak of 2003 (see Hilgenfeld and Peiris (2013), for a recent review), the genome of SARS-CoV was sequenced within three weeks of the discovery of the virus (Marra et al., 2003; Rota et al., 2003) and subjected to detailed annotation shortly thereafter (Snijder et al., 2003). At the same time and in subsequent years, leads for antiviral therapy were described (Anand et al., 2003; Yang et al., 2005; see Hilgenfeld (2014), for a recent review). However, the detailed molecular characterization of viral genome replication and the assembly of viral particles was initially restricted to specialized high-safety laboratories. This limitation was overcome by the finding that SARS-CoV replicons are able to replicate autonomously in transfected host cells (Almazán et al., 2006; Ge et al., 2007; Eriksson et al., 2008; Pan et al., 2008; Wang et al., 2008; reviewed in Almazán et al., 2014). Replicons, in particular those encoding a reporter gene, considerably facilitate the functional analysis of molecular determinants that control the replication and transcription of the SARS-CoV genome. SARS-CoV replicons consist of the genomic 5′ and 3′ untranslated regions and an open reading frame (ORF) encoding the two polyproteins (pp1a and, *via* a (-1) frame-shift, pp1ab) that are processed into 16 non-structural proteins (Nsp1 to Nsp16) to form the replication/transcription complex (RTC, Fig. 1A). Among the Nsps, Nsp3 is a multi-domain polypeptide comprising the following structurally organized domains (Serrano et al., 2009; Johnson et al., 2010): the ubiquitin-like domain 1 (UB1), the partially disordered acidic domain (Ac), the X domain, and the SARS-unique domain (SUD). This is followed by the second ubiquitin-like domain (UB2), which is usually considered part of the next domain, the papain-like protease (PL^{pro}). C-terminal to these, there is the nucleic-acid-binding domain (NAB), followed by a longer stretch of amino-acid residues apparently lacking secondary structure (occasionally called "coronavirus group 2 marker (G2M)"; Neuman et al., 2014) and the first transmembrane region (TM1). The zinc-finger (ZF) is the only domain on the

* Corresponding author.
E-mail addresses: koussov@biochem.uni-luebeck.de (Y. Kusov), tanjinzhi@gmail.com (J. Tan), ealvarezmba@gmail.com (E. Alvarez), L.enjuanes@cnb.csic.es (L. Enjuanes), hilgenfeld@biochem.uni-luebeck.de (R. Hilgenfeld).
[1] Present address: Centro de Biología Molecular Severo Ochoa. Consejo Superior de Investigaciones Científicas. Universidad Autónoma de Madrid (CSIC-UAM). Nicolás Cabrera 1, 28049 Madrid, Spain.

http://dx.doi.org/10.1016/j.virol.2015.06.016
0042-6822/

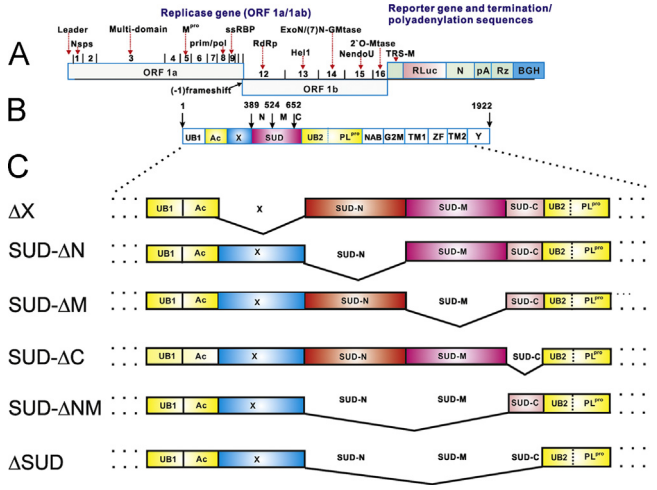

Fig. 1. Schematic presentations (not to scale) of the genetically engineered SARS-CoV replicon encoding Renilla luciferase (**A**), of the domain organization of Nsp3 (**B**), and of constructs with deleted fragments (ΔX, SUD-ΔN, SUD-ΔM, SUD-ΔNM, and SUD-ΔC) within domains X–SUD of Nsp3 (**C**). Nsp – nonstructural protein 1–16, M^{pro} – main (or 3C-like, 3CL) protease, prim/pol – non-canonical polymerase activity (Xiao et al., 2012; te Velthuis et al., 2012), ssRBP – single-stranded RNA-binding protein, RdRp – RNA-dependent RNA polymerase, Hel – superfamily-1 helicase, ExoN/(7)N-GMtase – 3′-to-5′ exonuclease/^{7}N-guanylmethyltransferase, NendoU – U-specific endoribonuclease, 2′O-Mtase – 2′O-methyltransferase, TRS-M – transcription-regulatory sequence of the M protein, RLuc – Renilla luciferase, N – nucleocapsid protein, pA – a synthetic poly(A) tail, Rz – hepatitis delta virus ribozyme, BGH – bovine growth hormone termination and polyadenylation sequence, UB1 – ubiquitin-like domain 1, Ac – acidic domain, X – X domain, SUD – SARS-unique domain, UB2 – ubiquitin-like domain 2 preceding the papain-like cysteine protease (PL^{pro}), NAB – nucleic acid-binding domain, G2M – coronavirus group 2 marker, TM1 and TM2 – transmembrane regions, ZF – zinc-finger, Y – uncharacterized domain. As shown schematically in panel C, Δ indicates a deletion of the X domain or of domains N, M, C, NM, or the complete SUD-coding sequences.

luminal side of the membrane; the second transmembrane region (TM2) and, finally, the uncharacterized Y domain are localized near the C-terminus of Nsp3 (Fig. 1B, see Neuman et al. (2014)).

The X domain was shown to have a macrodomain fold and proposed to be an ADP-ribose-1″-phosphate phosphatase (ADRP) or a poly(ADP-ribose)-binding module (Saikatendu et al., 2005; Egloff et al., 2006). We have shown previously that the SUD contains two consecutive macrodomains, called SUD-N and SUD-M (Tan et al., 2009). Although their functional role in the viral replication cycle remains unknown, we have shown that these macrodomains bind nucleic acids that contain long guanine stretches capable of forming G-quadruplexes (Tan et al., 2007, 2009).

In the present study, we investigated the X, SUD-N, and SUD-M macrodomains to determine whether they play important roles in viral genome replication/transcription and whether they act in *cis* or in *trans*. To this end, we have introduced in-frame deletions into the X and SUD regions of the SARS-CoV replicon, into which a reporter gene (Renilla luciferase, RLuc) was introduced under the control of the transcription regulatory sequence (TRS) for SARS-CoV structural protein M (Fig. 1A). In addition, the functional role of the SUD C-terminal region (SUD-C, a frataxin-like domain with as yet unknown function (Johnson et al., 2010)), was assessed in a similar way. The reporter gene-containing replicons were tested for their ability to support the activity of the RTC in the synthesis of subgenomic replicon RNA and to assess whether the deleted functions could be rescued *in trans*. The data presented indicate a crucial role for the SUD-M macrodomain for viral RTC activity, thus lending support to the significance of the previously observed binding of SUD to oligo(G)-containing nucleic acids (Tan et al., 2007, 2009). This observation was additionally reinforced by the analysis of replicons in which amino-acid mutations have been introduced in subdomains presumably involved in the interaction with G-quadruplexes (Tan et al., 2009).

Results

Introduction of deletions and point mutations into the SARS-CoV replicon encoding Renilla luciferase

Comparing genome transcription with genome replication, it was previously shown that the replicon pBAC-REP, which was lacking a reporter gene, was able to replicate in mammalian cells (Almazán et al., 2006). These data encouraged us to introduce a luciferase reporter gene into the replicon pBAC-REP to enable the quantitative detection of viral genome replication simply by measuring the luciferase activity. The Renilla luciferase was chosen as a reporter protein because of its longer half-life as compared to that of the firefly luciferase (see *Materials and methods* and Tanaka et al., 2012). However, the constructed full-length SARS-CoV replicon DNA, pBAC-REP-RLuc, was too large (approximately 33 kb) to ensure the correctness of desired deletions and/or mutations. Therefore, the engineered mutants lacking different genome fragments (complete SUD, or subdomains SUD-N, SUD-M, SUD-NM, and, finally, SUD-C, Fig. 1C) were first introduced by site-directed mutagenesis into the shorter plasmid pBAC-SfoI-MluI (approx. 15 kb, Supplementary Fig. 1B, Almazán et al., 2006). The fragments containing the deletions were then excised from these pBAC-SfoI-MluI-derived plasmids and transferred back into plasmid pBAC-REP-RLuc. To recover the replication/transcription activity, the correctly oriented MluI-MluI fragment was inserted into the final plasmids. Supplementary Fig. 1 depicts our main strategy exemplified by the construction of the SUD-deleted SARS-CoV replicon encoding Renilla luciferase as reporter protein (pBAC-ΔSUD-REP-RLuc).

To examine whether SUD function within the RTC might be connected to its binding to oligo(G)-stretches capable of forming G-quadruplexes (Tan et al., 2009), a SARS-CoV replicon containing the mutations K565A, K568A, and E571A within the SUD-M domain (referred to as the mut4 set of mutations) was constructed following a similar approach. We had shown previously that these mutations abrogate G-quadruplex binding to SUD-M (Tan et al. 2009). The replicon containing the mutations K476A and K477A (the mut2 set of mutations) located near the C-terminus of the SUD-N domain was also prepared for comparison, since these mutations had a weaker effect on SUD-oligo(G) binding according to zone-interference gel electrophoresis (Tan et al., 2009). To further test our hypothesis, the mutation sets mut2 and mut4 were also introduced into the replication-competent replicon pBAC-ΔX-REP-RLuc lacking the X domain (see below and Fig. 4A and B).

Replication-competence of the reporter gene-containing SARS-CoV replicon pBAC-REP-RLuc

To ensure that the reporter gene expression directly correlated with viral genome synthesis, the level of viral RNA synthesis was measured in parallel to Renilla luciferase activity. This was achieved by quantitative RT-PCR (qRT-PCR) using primers covering the non-structural protein 1 (Nsp1) region (see *Materials and methods*). There was a direct correlation of Renilla luciferase expression with the amount of viral RNA synthesis in mammalian cells transfected with the SARS-CoV replicon pBAC-REP-RLuc (Fig. 2A and B, columns “REP”). Due to the specificity of the forward and reverse primers, the qRT-PCR system gave a non-significant background (Fig. 2B, column “mock”). A replication-defective construct, pBAC-REP(NR)-RLuc, with a reverse

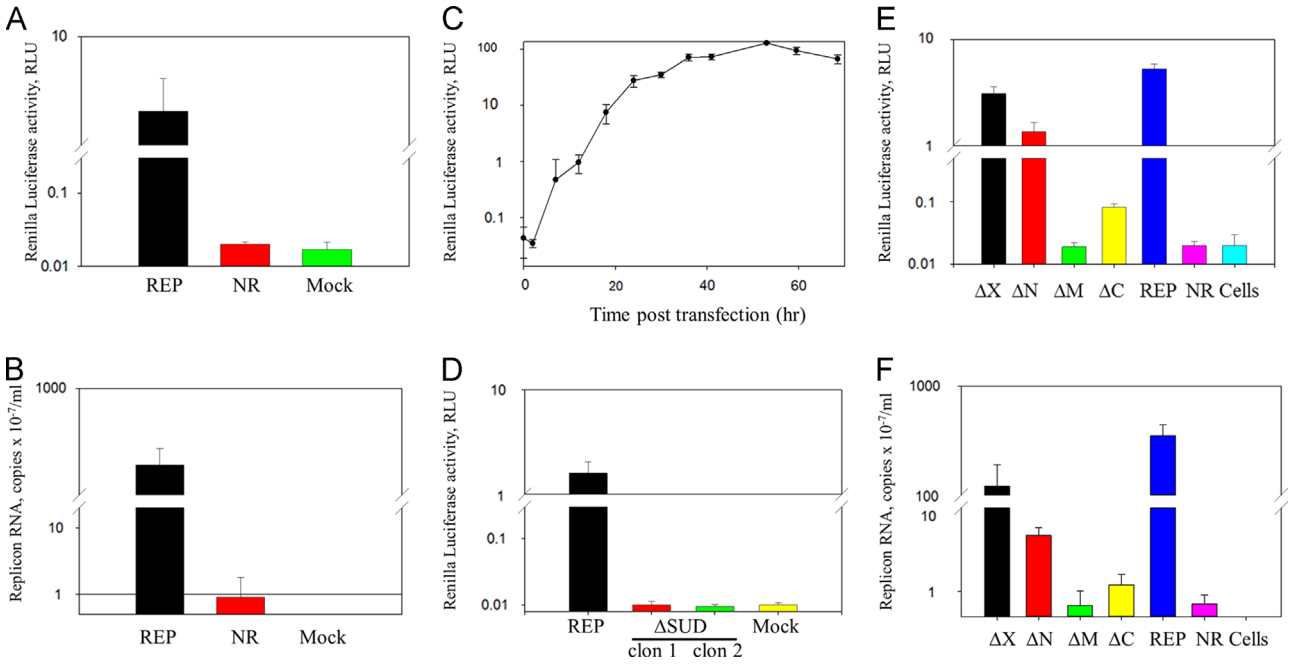

Fig. 2. Comparison of the level of Renilla luciferase expression (**A**) and viral RNA synthesis (**B**) by replication-competent (REP) and replication-deficient (NR) SARS-CoV replicons; time-course of RLuc expression by the SARS-CoV replicon (**C**); the effect of SUD deletion (two clones, clon1 and clon2) on Renilla luciferase expression (**D**), effect of deletion of the X domain (ΔX), SUD macrodomains (ΔN and ΔM), and of the SUD-C subdomain (ΔC) on the expression of Renilla luciferase (**E**) and on viral RNA synthesis (**F**). SARS-CoV replicons with deleted domains were transfected in Vero E6 cells and after 24 h of incubation, Renilla luciferase activity and the amount of viral RNA were measured (see *Materials and methods*). Renilla luciferase activity and viral RNA synthesis were also measured after transfection of a replication-deficient SARS-CoV replicon (NR) and in mock-transfected cells (Cells). Data shown are from quadruplicate experiments, expressed as the mean value of RNA copies ± standard deviation (SD). The difference in expression of the full-length SARS-CoV replicon and its various mutants was found to be significant, implying that values among them are greater than would be expected by chance ($0.01 > p > 0.001$). Note that in the replication-deficient SARS-CoV replicon (NR), the sequence of the MluI-MluI fragment is reversed, thus preventing the formation of the replicase complex. RLU – relative light units.

orientation of the MluI-MluI fragment used as a negative control, neither expressed Renilla luciferase nor was able to synthesize viral RNA (Fig. 2, A and B, columns "NR"). These results clearly indicate that Renilla luciferase activity is a good reporter for analyzing viral genome replication.

To find out the optimum time for the reporter-gene expression by the engineered SARS-CoV replicon, the Renilla luciferase activity was analyzed at different time-points after transfection of pBAC-REP-RLuc into Vero E6 cells. As shown in Fig. 2C, the reporter gene expression showed a linear increase between 18 and 53 h posttransfection (hpt), with the highest value of Renilla luciferase activity detected around 53 hpt. Therefore, the expression between 24 and 48 hpt was recorded in our study.

The X macrodomain of SARS-CoV is dispensable for RTC activity

A few regions near the 5′ end of the coronavirus genome (nsp1 of murine hepatitis virus, MHV (Denison et al., 2004; Brockway and Denison, 2005, Tanaka et al., 2012), and nsp2 of MHV and SARS-CoV (Graham et al., 2005)) have been shown to be dispensable for virus replication (reviewed in Neuman et al., 2014). In addition, the ADRP of Nsp3b, *i.e.* the X domain of human coronavirus 229E (HCoV 229E) can be inactivated by mutation without significantly affecting viral replication in cell culture (Putics et al., 2005). To find out whether the X domain may display another, as yet uncharacterized activity involved in viral replication or transcription, we removed the coding sequence for the complete domain from the SARS-CoV replicon and found that the resulting replicon, pBAC-ΔX-REP-RLuc, was replication-competent. Approximately 70–75% of the parental replicon (pBAC-REP-RLuc) activity (Fig. 2E, column "REP") was observed for the expression of the X domain-deleted replicon (Fig. 2E, column "ΔX"). To ensure that the reporter-gene expression correlated with viral genome synthesis, Renilla luciferase activity expressed by constructs lacking individual domains (in this case the X domain) was directly compared with RNA synthesis. A high level of viral RNA synthesis was observed for the X-domain-deleted construct (Fig. 2F, column "ΔX"). Thus, not only is the ADRP activity of the X domain not required for coronavirus replication in tissue culture, as shown for HCoV 229E (Putics et al., 2005), but the entire X domain is dispensable in case of SARS-CoV (our data).

SUD is indispensable for SARS-CoV genome transcription/replication

In case of the SUD, we have shown that it preferentially binds oligo(G) stretches (G-quadruplexes) (Tan et al., 2007, 2009). To assess the importance of SUD for the activity of the RTC, the entire SUD-encoding sequence was deleted from the SARS-CoV replicon, as described above. The ability of the deleted construct pBAC-ΔSUD-REP-RLuc to replicate its genome was compared to that of the parental replicon pBAC-REP-RLuc. In contrast to the latter (Fig. 2D, column "REP"), two independently prepared clones of pBAC-ΔSUD-REP-RLuc, transfected in Vero E6 cells, expressed the Renilla luciferase gene only at a level similar to background activity, suggesting that the SUD is indispensable for SARS-CoV RTC activity (Fig. 2D, *cf.* columns "ΔSUD" with column "mock").

Lack of trans-complementation of the replication-deficient SUD-lacking SARS-CoV replicon by the full-length SUD and SUD-NM

To answer the question whether the SUD function is required exclusively in *cis* or can be provided in *trans*, the full-length SUD or its more stable SUD-NM fragment was co-transfected together with the SUD-deleted replicon pBAC-ΔSUD-REP-RLuc in Huh-T7 cells susceptible to SARS-CoV (Gillim-Ross et al., 2004;

Hattermann et al., 2005). However, the reporter gene activity did not exceed background level (Fig. 3, panel A). None of the constructs expressing SUD or SUD-NM (columns 2 and 3, respectively) was able to considerably enhance the extremely low reporter gene activity of the SUD-lacking replicon co-transfected with vector alone (column 1). Intriguingly, the co-expression of SUD or SUD-NM with the replication-competent SARS-CoV replicon (REP-RLuc, columns 5 and 6, respectively) slightly inhibited the Renilla luciferase activity expressed by the replicon co-transfected with the vector pIVEX used as a control (column 4). Assuming that the inability to complement the SUD-deleted replicon by providing SUD or SUD-NM in *trans* was due to low levels of protein production, we increased the amount of expression using vaccinia virus (VV) MVA-T7 as a helper virus. Previously, we have successfully used MVA-T7 to efficiently express hepatitis A virus genes (Kusov et al., 2002). Indeed, the transfection of constructs expressing SUD or SUD-NM followed by infection with the helper virus MVA-T7 (a procedure known as transinfection, Kusov et al., 2002) allowed immunological detection of SUD and SUD-NM using either polyclonal SARS-CoV anti-Nsp3 (Rockland; result not shown) or monoclonal anti-His_4 (Qiagen) (Fig. 3C). Note that the level of Renilla luciferase expression by the SUD-deleted replicon was also increased, probably because of more efficient mRNA transcription from a cryptic promoter or due to a helper effect of VV for replicon RNA synthesis, as we and others have noticed previously (Sutter et al., 1995; Kusov et al.,

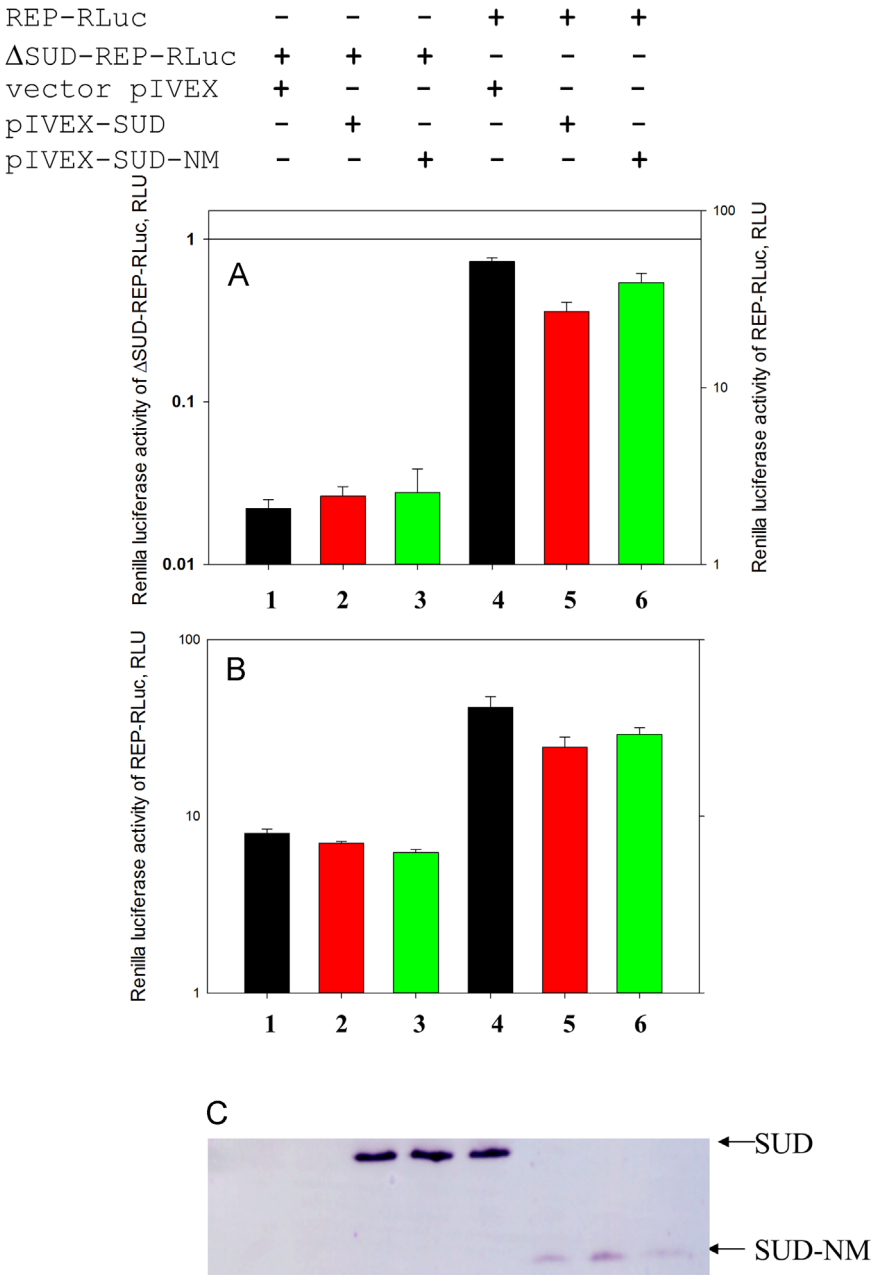

Fig. 3. Impact of SUD and SUD-NM proteins, provided *in trans*, on the activity of the full-length and SUD-deleted SARS-CoV replicons. Indicated DNAs were co-transfected in Huh-T7 cells (**A**) or additionally infected with vaccinia virus MVA-T7 as a helper virus (see *Materials and methods*) (**B**). The infection and/or co-transfection mixtures were replaced with growth medium and incubated for an additional 48 h. The cell lysates were analyzed for Renilla luciferase (A and B, $p < 0.01$) and anti-His immunological activity in mixtures 2 and 3 shown in panel B (**C**). All experiments were run in triplicate and the average was employed for analysis. Error bars represent standard deviations of the mean values. The difference in reporter protein activity of the full-length replicon and the SUD-lacking replicon was found to be statistically significant (panel A, $p=0.005$; panel B, $p=0.01$).

2002). However, none of the proteins, SUD (Fig. 3B, column 2) or SUD-NM (column 3), was able to increase the reporter-gene expression of the SUD-deleted replicon pBAC-ΔSUD-REP-RLuc (column 1), indicating that the function(s) of SUD cannot be complemented in *trans*. To double-check these results, we have tried to supplement the parental SARS-CoV replicon pBAC-REP-RLuc. In line with the data presented in Fig. 3A, the co-expression of SUD or SUD-NM rather partially inhibited the Renilla luciferase activity of the replication-competent replicon (Fig. 3, *cf.* columns 4 and 5 in panels A and B), implying that possibly a fine balance of the proteins is crucial for the formation of the active SARS-CoV replicase complex. Taken together, the functional activity of SUD in *cis* could not be supplemented in *trans*, neither by the full-length SUD nor by its more stable version SUD-NM consisting of the two macrodomains, SUD-N and SUD-M.

The SUD-M macrodomain is crucial for the activity of the replication/transcription complex

To assess the role of the subdomains of SUD for the activity of the RTC, the SUD-N and SUD-M macrodomains and the C-terminal subdomain (SUD-C) were deleted in separate experiments from the sequence of the SARS-CoV replicon (Fig. 1). We compared the activities of the replicons lacking individual SUD subdomains to that of the parental SARS-CoV replicon, pBAC-REP-RLuc. The SARS-CoV replicon lacking the SUD-N domain expressed 30 to 35% of the Renilla luciferase activity of the parental replicon (Fig. 2E, column "ΔN"). Accordingly, its RNA level was well detectable in contrast to other SUD subdomain-deleted replicons (Fig. 2F, compare the column "ΔN" with those for ΔM and ΔC). These data indicate that the SUD-N macrodomain may also be considered dispensable for SARS-CoV replication, similar to the X domain (see above), although their effects on replication may be considered "minor" (X domain) and "moderate" (SUD-N domain), respectively. In sharp contrast, the Renilla luciferase activity expressed by the replicon with the SUD-M domain deleted (Fig. 2E, column "ΔM") did not exceed the level of the activity expressed by the replication-deficient replicon pBAC-REP(NR)-RLuc (Fig. 2E, column "NR"). This activity was similar to the background level detected in mock-transfected cells (Fig. 2E, column "Cells"). The lack of replication of the SUD-M domain-deleted replicon, deduced from the negligible level of Renilla luciferase activity, was confirmed by quantification of the viral genome (Fig. 2F, column "ΔM"). The pBAC-SUDΔC-REP-RLuc replicon was able to replicate only to a significantly lower extent than the construct lacking the SUD-N domain (Fig. 2, E and F, *cf.* columns "ΔC" and "ΔN"). Nevertheless, its Renilla luciferase expression and the synthesis of viral RNA were always at detectable levels (Fig. 2, E and F, columns "ΔC"), in contrast to the activity of the SUD-M-lacking replicon (column "ΔM") or to that of the replicon with the SUD-NM domains deleted (not shown). The RTC activity of the latter replicons was either at background level (columns "Cells") or at the level of the replication-deficient construct (columns "NR"). In summary, among all tested SARS-CoV replicons with the above-mentioned deletions, the replication ability was mostly affected by the deletion of the SUD-M macrodomain.

Charged amino-acid residues of the SUD-M macrodomain presumably involved in G-quadruplex binding are essential for SARS-CoV RTC function

Among all previously tested sets of amino-acid replacements that were able to affect the binding of SUD to G-quadruplexes, the mut4 set of mutations, comprising alanine substitutions of K565, K568, and E571 of Nsp3, was most efficient in preventing the binding of oligo(G) (Tan et al., 2009). These amino-acid residues are located in the loop connecting the second α-helix with the third β-strand of the SUD-M domain, which was found to be essential for replication of the SARS-CoV replicon (Fig. 2E and F). In contrast, the mutations K476A and K477A (the mut2 set of mutations) located in the dispensable SUD-N domain (Fig. 2E and F) had only a minor effect on oligo(G)-binding *in vitro* (Tan et al., 2009).

To compare the effect of mutations on viral genome replication/transcription *in vivo*, the two sets of mutations (mut2 and mut4) were introduced separately into two SARS-CoV replicons containing the full-length SUD sequence, pBAC-REP-RLuc and pBAC-ΔX-REP-RLuc, which were able to efficiently replicate their genome as judged by Renilla luciferase expression and viral RNA synthesis (Fig. 2). A replicon lacking the SUD-C subdomain, pBAC-SUDΔC-REP-RLuc, which contains both the SUD-N and SUD-M domains, was not considered for site-directed mutagenesis because of its low activity.

The impact of the mut2 and the mut4 set of mutations on the activity of the RTC was examined by reporter gene expression and viral RNA synthesis as mentioned above. Compared to the original constructs, the non-mutated replicon pBAC-REP-RLuc (Fig. 4A) and its X domain-deleted derivative pBAC-ΔX-REP-RLuc (Fig. 4B), the corresponding replicons containing the mut2 set of mutations (K476A and K477A) expressed Renilla luciferase activity three times more weakly (Fig. 4A, -SUDmut2-), or even at the same level (Fig. 4B, -ΔX-SUDmut2-). Probably, this difference is connected with the reduced activity of the SARS-CoV replicon lacking the X domain (see Fig. 2E and F). In contrast to the effect of mut2 variants, the Renilla luciferase activity of replicons containing the mut4 set of mutations was negligible, thereby emphasizing the crucial role of the residues altered in the mut4 set of mutations for genome replication (Fig. 4A and B, -SUDmut4- and -ΔX-SUDmut4-). These results were in close agreement with the levels of quantified viral RNA (not shown). Taken together, the effect of charged amino-acid residues on the *in-vitro* binding of SUD-NM to G-quadruplexes strictly correlated with the activity of the mutated SARS-CoV replicons *in vivo*.

Discussion

The highly infectious and virulent Severe Acute Respiratory Syndrome coronavirus (SARS-CoV), classified as a biosafety level-3 agent (BSL3), can only be handled in specially equipped laboratories. To overcome this limitation and to avoid the use of dangerous live virus, SARS-CoV replicons have been engineered (Almazán et al. 2006, 2014; Ge et al., 2007; Eriksson et al., 2008; Pan et al., 2008; Wang et al., 2008). Here, we have constructed a SARS-CoV replicon containing Renilla luciferase as reporter gene, thus allowing not only the easy screening of chemical libraries for antivirals interfering with replication of viral RNA and the characterization of antiviral lead compounds, but also studies of the function of various viral proteins and regulatory sequence elements by reverse genetics.

Our aim was to elucidate the functional role of the three sequential macrodomains within Nsp3 for the activity of the SARS-CoV RTC. To this end, we have created various SARS-CoV replicons with deleted and/or mutated macrodomains. First, the X domain-encoding sequence was deleted from the Renilla luciferase-containing SARS-CoV replicon and the resulting replicon was tested for its ability to express the reporter gene. The X domain has been shown to exhibit a weak ADRP activity in most coronaviruses examined, but we have previously shown that this activity is not completely conserved across the family; thus, the X domain of the Beaudette strain of Infectious Bronchitis Virus (IBV) is unable to bind ADP-ribose due to replacement of a Gly-Gly-Gly

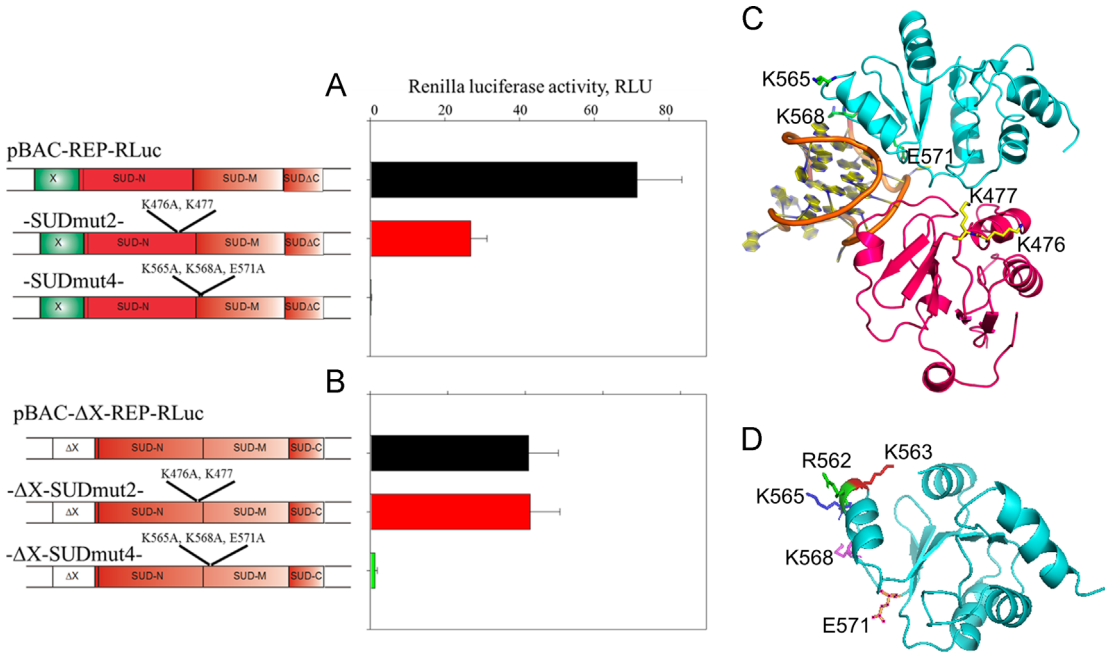

Fig. 4. Effect of amino-acid replacements in the SUD macrodomains on viral genome transcription/replication. Indicated mutations in SUD-N and SUD-M (designated –SUDmut2- and -SUDmut4-, respectively) were introduced into the SARS-CoV replicon pBAC-REP-RLuc (**A**) and its derivative lacking the X domain, pBAC-ΔX-REP-RLuc (**B**) (see diagrams at the right side of the constructs). The ability of the constructs to exhibit Renilla luciferase activity is presented as mean values of triplicate experiments ± SD ($p < 0.05$). A putative model of G-quadruplex binding to SUD-NM, obtained by automated docking into the crystal structure (**C**, modified from Tan et al., 2009). The SUD-N and SUD-M macrodomains are in violet and cyan, respectively. The G-quadruplex as found in the BCL2 promoter region (PDB code: 2F8U, Dai et al., 2006) is in orange. The mut2 set of mutations (K476A + K477A), located at the C-terminus of the SUD-N domain, is indicated by yellow sticks. The mut4 set of mutations (K565A + K568A + E571A), of SUD-M, is indicated by green sticks. These residues belong to a cluster of charged amino-acid residues located in the second α-helix of SUD-M and in the loop connecting it with the third β-strand (R562, K563, K565, K568, and E571, green, red, blue, magenta, and orange label, respectively) (**D**).

triplet in the binding site by Gly-Ser-Gly (Piotrowski et al., 2009). Furthermore, Putics et al. (2005) reported that the ADRP activity of HCoV 229E is not essential for genome replication of this virus in cell culture. In this study, we find that the replicon pBAC-ΔX-REP-RLuc expressed a high level of Renilla luciferase and was able to synthesize viral RNA after transfection into mammalian cells (Vero E6 or Huh-T7, a derivative of SARS-CoV-susceptible Huh-7 cells (Gillim-Ross et al., 2004; Hattermann et al., 2005)). This indicates that the X domain does apparently not carry another, as yet unidentified, activity that would be essential for SARS-CoV replication/transcription. In sharp contrast to results with the deleted X domain, the SUD-lacking replicon, pBAC-ΔSUD-REP-RLuc, abrogated reporter gene expression and the synthesis of viral RNA (Fig. 2D and not shown, respectively). To our knowledge, this is the first description of the indispensability of SUD for SARS-CoV genome replication. The most plausible explanation for this observation is an essential role of the SUD-M macrodomain for viral RNA synthesis (see below).

Interestingly, all our attempts to complement *in trans* the SUD function by co-expression of the full-length SUD or SUD-NM failed, albeit the expression was evidenced by immunological detection of the proteins (see Fig. 3). Also, the replication of the complete SARS-CoV replicon was not enhanced when a full-length SUD or SUD-NM were provided *in trans* (Fig. 3). The inability to supply SUD activity *in trans* rules out a hypothetical enzymatic activity of SUD. Taken together, these results indicate that the functionally active SUD is required only *in cis* or, alternatively, a fine balance of the proteins is essential for the formation of the active SARS-CoV replicase complex. These observations may substantiate the previously published data on enhancement of SARS-CoV reporter activity by the co-expression of Nsp3.1, which comprises domains X and SUD (Pan et al., 2008). Now we can assume that this enhancement was mainly due to the presence of the X domain within Nsp3.1. Alternatively, the three sequentially positioned macrodomains, *i.e.* X, SUD-N, and SUD-M, may have (an) as yet unidentified function(s) enhancing SARS-CoV genome replication. Since full-length SUD was found to be crucial for SARS-CoV genome replication (Fig. 2D) and not able to complement *in trans* (Fig. 3), we decided to gain further insight into the role of each SUD macrodomain for RTC activity. In addition, the C-terminal SUD subdomain (SUD-C) was also investigated by removal of the SUD-C-coding sequence from the SARS-CoV replicon. The deletion of the SUD-M domain completely abolished both replicon activities, thus indicating that the SUD-M domain is indispensable for SARS-CoV genome replication. In contrast, the SUD-N domain was revealed to be non-essential for RTC activity since its removal abolished neither Renilla luciferase expression nor viral RNA synthesis (Fig. 2, E and F, columns "ΔN"). The same is true for the SUD-C subdomain, although the RTC activity of the SUD-C-lacking replicon was always at a low level (Fig. 2, E and F, columns "ΔC"). Intriguingly, three amino-acid residues (K565, K568, and E571) located in the loop following the second α-helix of SUD-M and responsible for the interaction of SUD with oligo(G)-nucleotides have previously been identified (Tan et al., 2009). We propose that the SUD-oligo(G) interaction is required for SARS-CoV genome replication. The SARS-CoV genome contains a number of conserved G_4 stretches (Johnson et al., 2010) that could be binding-partners for SUD. Oligo(G) sequences are capable of forming G-quadruplexes, even if they comprise a few non-guanines; thus, the NMR structure of the prototype G-quadruplex that we used for docking into the SUD-NM cavity contains 8 non-guanines among 23 nucleotides (Dai et al., 2006). Therefore, oligo (G) regions such as, *e.g.*, 5′-GGGAGGUAGG-3′, which is found conserved in the Nsp2- and Nsp12-coding regions in the genomes of different SARS-CoV strains (Johnson et al., 2010), are candidates for interaction with SUD.

While these observations support an essential role of the SUD-M domain in replication/transcription of the SARS-CoV genome,

probably *via* interaction with G-rich stretches forming G-quadruplexes, we have to consider a potential negative effect of SUD domain deletions on the activity of the papain-like protease (PL^{pro}), located immediately downstream of SUD. Such a modulation of PL^{pro} activity by flanking regions has been reported for SARS-CoV PL^{pro} (Harcourt et al., 2004; Han et al., 2005) and alphacoronavirus $PL2^{pro}$ (Ziebuhr et al., 2001, 2007). Therefore, to demonstrate a direct correlation between the G-quadruplex interaction and the replication ability of SARS-CoV replicons and to exclude a possible modulating effect of domains preceding the PL^{pro}, we reasoned to leave the SUD intact but mutate the amino-acid residues putatively involved in SUD-binding to G-quadruplexes. The replacement of charged amino-acid residues by alanine (K565A, K568A, and E571A, mut4 set of mutations) on the surface of the SUD-M domain that is oriented towards the SUD-N domain and remote from the PL^{pro} (Tan et al., 2009), completely abrogated the Renilla luciferase expression (Fig. 4) and the synthesis of viral RNA (not shown), both in the context of the SARS-CoV replicon and its X-lacking version. In contrast, and consistent with the previously described marginal effect of the lysine residues at positions 476 and 477 of the SUD-N domain on G-quadruplex-binding *in vitro* (Tan et al., 2009), the introduction of the mut2 set of mutations (K476A and K477A) into the above-mentioned replicons had only a minor effect on expression of Renilla luciferase (Fig. 4) and viral RNA synthesis (not shown). In agreement with this, the replicon with the SUD-N domain deleted was able to replicate (Fig. 3E and F, columns "ΔN").

These results were consistent with our hypothesis that SARS-CoV genome replication requires the interaction of SUD with oligo (G)-containing nucleic acids (Tan et al., 2007, 2009). Amino-acid replacements (mut4), which in *in-vitro* experiments abrogated the interaction of mutated SUD-NM with oligo(G) (Tan et al., 2009), resulted in a replication-defective construct. In contrast, the mut2 set of mutations with negligible effect on oligo(G)-binding to SUD-NM *in vitro* (Tan et al., 2009) resulted in a viable replicon.

Taken together, these data suggest SUD amino-acid residues that are strictly required for SARS-CoV genome replication. These residues (lysine residues 565, 568, and glutamate 571) are located in the loop connecting the second α-helix with the third β-strand of the SUD-M macrodomain; interestingly, the two lysine residues belong to a region shown to be involved in G_{10}-binding by NMR-shift perturbation analysis (Johnson et al., 2010) and are involved in interactions with a G-quadruplex according to our docking model (Fig. 4C and D). Considering their electrostatic potential, the replacement of these amino-acid residues by alanine will affect the charge distribution within the binding site for G-quadruplexes or other nucleic acids (Supplementary Fig. 2 and Supplementary text B). Such a modification of the binding site's electrostatic potential results in abrogation of the SUD – nucleic-acid interaction (Tan et al., 2009) that is required for SARS-CoV genome replication in a cell-based assay (Supplementary Fig. 2). On the other hand, the replacement of lysine by alanine at positions 476 and 477 did not significantly affect either the electrostatic potential of the binding site (Supplementary Fig. 2) or the direct interaction with the G-quadruplex (Fig. 4C). Although we did not construct the replicon containing arginine to alanine replacement at position 562, we speculate that this highly conserved arginine residue is also involved in G-quadruplex binding, since it is located in close proximity to the binding cavity (Supplementary Fig. 3 and Fig. 4D; R562, green label) and has also been identified as part of the nucleic-acid binding site in the NMR-shift perturbation experiments reported by Johnson et al. (2010). In contrast, the lysine residue at position 563 seems to be oriented away from the binding pocket (Fig. 4D; K563, red label), thereby preventing its participation in oligo(G) interaction. The participation of the strictly conserved E571, which is located close to the binding site but negatively charged (Fig. 4D, orange label, and Supplementary Fig. 3) needs to be further investigated. In summary, we have identified amino-acid residues essential for SARS-CoV genome replication, which requires SUD-oligo(G) interaction. Interestingly, this cluster of charged amino-acid residues located in the second α-helix of the SUD-M domain, or in the loop following it (Fig. 4D; R562, K565, K568, and E571, green, blue, magenta, and orange labels, respectively), is conserved among established human SARS-CoV strains (Urbani, Frankfurt, Tor2, GZ02, and BJ01) and SARS-CoV-related bat and civet isolates (RsSHC014, RS3367, Rs672/2006, HKU3-1, Rf1, Rm1, Rp3, SZ3, SZ16, Bat273, Bat 279, and BM48) (Supplementary Fig. 3).

Despite strong evidence for SUD-M domain - G-quadruplex interaction demonstrated *in vitro* (Tan et al., 2007, 2009) as well as *in vivo* (this work), we do not rule out a role in replication of other possible SUD functions, such as the SUD-SUD, SUD-UB1, and SUD-X domain-domain interactions described previously (Neuman et al., 2008). Nevertheless, supporting a crucial role for oligo(G)-binding in viral genome replication, a similar, but not identical, stretch of charged amino-acid residues was also found to be conserved in the genome of the newly emerging human Middle-East Respiratory Syndrome coronavirus (MERS-CoV) and in the genomes of the closely related bat CoVs, HKU4 and HKU5, as well as in the genome of CoVs isolated from dromedars, which are supposed to be a primary animal reservoir of MERS-CoV (Memish et al., 2014) (see Supplementary Fig. 3). Intriguingly, as seen for the SUD-M macrodomain, we found the putative M domain of MERS-CoV to bind exclusively oligo(G) (and not oligo(A), oligo(C), or oligo (U)) nucleotides (Lei et al., personal communication). It is highly probable that this property is attributable to the stretch of conserved charged residues on the surface of the M domain of MERS-CoV (see Supplementary Fig. 3). Further studies will be required to elucidate the impact of the deletions and mutations described here at the level of the full-length SARS-CoV genome and, in particular, to answer the question whether any second-site mutation(s) can rescue the mutated virus.

Conclusion

In this contribution, we demonstrate, for the first time, the functional role of the SUD subdomains within the replication–transcription activity of the Severe Acute Respiratory Syndrome Coronavirus (SARS-CoV). Contrary to the dispensable SUD-C and SUD-N subdomains as well as to the X domain preceding SUD in the genome, the SUD-M macrodomain was found to be crucial for the activity. The indispensability of this subdomain might be connected with its ability to bind oligo(G) stretches/G-quadruplexes as concluded from the results of site-directed mutagenesis of charged amino-acid residues in the loop connecting the second α-helix of SUD-M with the third β-strand. Intriguingly, a similar, but not identical, cluster of residues is observed in the genomes of the newly emerging human Middle-East Respiratory Syndrome coronavirus (MERS-CoV), MERS-related dromedary camel CoV, and bat CoVs HKU4 and HKU5.

Materials and methods

Cells and viruses

African green monkey kidney cells (Vero E6) and Huh-T7 cells, a derivative of human hepatocellular carcinoma Huh-7 cells (Nakabayashi et al., 1984) that constitutively expresses the T7 RNA polymerase (Shultz et al., 1996), were grown in Dulbecco's modified minimal essential medium (DMEM) supplemented with

2 mM glutamine, 100 U/ml penicillin, 100 μg/ml streptomycin sulfate, and fetal calf serum (10% v/v). Huh-T7 cells were additionally supplemented with geneticin (G-418 sulfate, 400 μg/ml). The recombinant, non-cytopathic vaccinia virus (VV) MVA-T7 was used to produce SUD or its subdomains N+M (SUD-NM) in order to complement *in trans* the activity of the SARS-CoV replicon lacking SUD. MVA-T7 was propagated in BHK-21 baby hamster kidney cells and titrated as described previously (Kusov et al., 2002). Other cell and culture conditions have been described in Almazán et al. (2006) and Kusov et al. (2006).

Construction of the SARS-CoV replicon containing reporter gene

To generate a SARS-CoV replicon containing a reporter gene, we have taken advantage of the strategy previously described for the construction of a SARS-CoV replicon lacking a reporter gene (Almazán et al., 2006). A Renilla luciferase as a reporter gene (RLuc, *Renilla reniformis*, also known as sea pansy) was PCR-amplified using pRL-SV40 DNA as a template (Promega; acc. AF025645), forward and reverse primers (Supplementary Table 1), and proof-reading DNA polymerase (AkkuPrime Pfx SuperMix, Invitrogen). The transcription regulatory sequence for the SARS-CoV M protein (TRS M) and a Kozak sequence enhancing expression in eukaryotic cells were included in the forward RLuc primer (Almazán et al., 2004; Kozak, 1989). The PCR amplicon was treated with AscI and BamHI and introduced between the same restriction sites of the SARS-CoV replicon pBAC-REP-URB (Almazán et al., 2006) producing the reporter gene (RLuc)-containing SARS-CoV replicon, referred to as pBAC-REP-RLuc (Supplementary Fig. 1). To exactly conform to the Kozak sequence, the second amino-acid residue of Rluc (tyrosine) was replaced by alanine. This replacement was successfully employed in the RLuc expression vector pBS-35S-Rluc-Ala (acc. number AY189983).

Introduction of deletions and point mutations into the Renilla gene-containing SARS-CoV replicon

All desired deletions and point mutations were introduced into the pBAC-REP-RLuc plasmid encoding polyproteins pp1a and pp1ab as replicase and RLuc as reporter protein (see above). However, to simplify the cloning procedure, we used as template for site-directed mutagenesis the shorter plasmid pBAC-SfoI-MluI encoding only the N-terminal half of polyprotein 1a (Nsp1–Nsp3) of SARS-CoV (Almazán et al., 2006). In brief, a Phusion Hot Start DNA polymerase (Phusion Site-Directed Mutagenesis Kit, Finnzymes), which ensures high fidelity for the amplification of large plasmids, was employed to extend perfectly matched 5′-phosphorylated forward and reverse primers (Supplementary Table 1) that border the deleted area as schematically exemplified in Supplementary Fig. 1B for deletion of the complete SUD sequence. The amplification mixture was treated with DpnI to destroy the original template DNA and the amplicon was circularized with Quick T4 DNA ligase (Finnzymes). An aliquot of the ligation mixture was transformed by electroporation (2.5 kV, 200 Ω, 25 μF) into electrocompetent *E. coli* cells (DH10B, NEB 10-beta, New England Biolabs) or HST02 (Takara) that are suitable for transformation of long-size plasmids. Positive clones were initially identified by restriction analysis and then confirmed by sequencing. An agarose gel-purified SfoI-ΔSUD-MluI fragment was transferred into dephosphorylated pBAC-REP-RLuc (Supplementary Fig. 1A) that was restricted with SfoI and MluI. For this procedure, the DNA ligase ⟨long⟩ optimized for cloning large DNA fragments was used as recommended by the manufacturer (Takara). The efficiency of transformation was tremendously increased after removing components of the ligation buffer by sodium acetate/ethanol precipitation. The resulting SUD-lacking plasmid (ΔSUD), which encoded the Renilla luciferase reporter gene, was still replication-deficient because of the absence of the MluI-MluI fragment. To restore all replicase components, this fragment was re-introduced at the MluI recognition site according to the procedure for cloning long DNA fragments (see above). The correct orientation of the MluI-MluI fragment was proven by StuI digestion prior to sequencing. The plasmid with reverse orientation of the MluI-MluI fragment was used as negative, non-replicating (NR) control.

A similar cloning strategy was employed to introduce point mutations into the replicon pBAC-ΔX-REP-RLuc lacking the X domain and into the full-length replicon pBAC-REP-RLuc. Two sets of mutations – K476A and K477A (mut2) in the SUD-N domain and K565A, K568A, and E571A (mut4) in the SUD-M domain – were introduced into both replicons. Phosphorylated asymmetric forward and reverse primers overlapping only within a short sequence (Supplementary Table 1) were employed for site-directed mutagenesis as described above. Mut2- and mut4-containing clones were identified by BtsI and BstAPI digestion, respectively. The ORF of all constructed SARS-CoV replicons bearing deletions or mutations within Nsp3, schematically depicted in Fig. 1C (ΔSUD, ΔX, SUD-ΔN, SUD-ΔM, SUD-ΔNM, and SUD-ΔC replicons) and Fig. 4 (-SUDmut2- and -SUDmut4-, -ΔX-SUDmut2- and -ΔX-SUDmut4-), was verified by complete sequencing of SfoI-MluI fragments (LGC Genomics). Details of the cloning procedures, restriction analysis of constructed plasmids, their maps and sequences can be provided upon request.

Transfection of SARS-CoV replicons in Vero E6 or Huh-T7 cells

Grown in twelve-well plates to 95% confluence, Vero E6 or Huh-T7 cells (1×10^5 cells/well) were transfected with deleted or mutated SARS-CoV replicons by using Lipofectamin 2000 according to the manufacturer's specifications (Invitrogen). At indicated time-points (see figure legends), the cells were lysed and the Renilla luciferase activity and/or viral RNA genome was measured in cell lysates (see below). All experiments were performed in triplicate or quadruplicate and the mean values and standard deviations (SD) are presented. Plasmid pRL-SV40 DNAs (Promega, acc. AF025645) and the wild-type SARS-CoV replicon were applied as control reporters in all transfection experiments.

Assay of Renilla luciferase activity

To lyse the cells, 150 μl/well of Passive lysis buffer (Promega) was added to the washed cell monolayer in 12-well plates (1 ml/well, phosphate-buffered saline, PBS) and incubated for 20 min at room temperature (RT) with rigorous shaking. The cells were further lysed by a freeze (−80 °C) / thaw procedure, vortexed, and centrifuged (18,400 × *g*, 1 min). To a 20-μl aliquot of clear supernatant, a mixture of Renilla luciferase assay and enhancer solutions (50 μl each, Biotium) was added and the luminescence was immediately measured using an Anthos Lucy-3 luminescence plate reader (Anthos Labtec Instruments). Data presented in Figs. 2, 3, and 4 are from quadruplicate experiments and are expressed as the mean value ± standard deviation (SD). The differences in Renilla luciferase expression of the full-length SARS-CoV replicon and its various mutants were analyzed with Sysstat (SigmaPlot Software Inc.) and found to be statistically significant implying that values are greater than would be expected by chance.

Viral RNA quantification

To isolate the viral RNA from Vero E6 cells transfected with SARS-CoV replicons containing deletions or mutations, the cells

were trypsinized as usual and spun down (1000 × *g*, RT, 5 min). The cell pellet was washed with PBS and cells were suspended in 100 μl PBS before dividing into two aliquots. A 20-μl aliquot of cell suspension was used for the evaluation of Renilla luciferase activity after lysis of pelleted cells in 50 μl Passive lysis buffer as described (see above). The total RNA was isolated from 80 μl of cell suspension using the RNeasy extraction kit and DNaseI treatment as recommended by the supplier (Qiagen). Trace amounts of DNA were removed from RNA preparations (20 μl) by additional treatment (37 °C, 30 min) with 1 unit of RNase-free DNase I in DNase buffer containing $MgCl_2$. The DNase was inactivated by adding 1 μl of 25 mM EDTA solution and heating at 65 °C for 10 min. The yield of total RNA was quantified by using a NanoDrop 1000 UV/Vis spectrophotometer (Thermo Fisher). An equal amount (500 ng) of RNA samples extracted from cells transfected with deleted SARS-CoV replicons was directly used as template for the first-strand cDNA synthesis. The reaction mixture (25 μl) additionally containing a reverse ΔX primer (200 nM, see Supplementary Table 1) and all four standard dNTPs (800 μM each) was pre-incubated at 65 °C for 5 min, chilled on ice to destroy any secondary structure of viral RNA and, after addition of RNase inhibitor (1 μl, Ribolock, Thermo Scientific) and reverse transcriptase (40 units, Thermo Scientific), further incubated at 45 °C for 60 min. The reverse transcriptase was inactivated by incubation at 70 °C for 5 min. A similar mixture without reverse transcriptase was used as a control. A 5-μl aliquot of the mixture was used for Real-Time PCR after addition of forward and reverse primers (0.3 μM each, see Supplementary Table 1; note that these primers represent a sequence of Nsp1 allowing to determine genome replication, but not transcription), a fluorescence-quenching primer (6FAM-ACCATCAAGTATGGTGA-CAGCTGCTCT-BBQ, 0.2 μM; TIB MolBiol), and a Maxima Probe qPCR Master Mix (Fermentas, MBI) in a total volume of 20 μl. A calibration curve was prepared by $\log_{10}$ dilution of pBAC-REP-RLuc in nuclease-free water. The measurements were performed in triplicate or quadruplicate; mean values of genome copies and SD are presented. Data shown are from quadruplicate experiments, expressed as the mean value of RNA copies ± standard deviation (SD). The statistical analysis of RNA copies for the full-length SARS-CoV replicon and mutants was performed as described above.

Generation of plasmids to express full-length SUD and SUD-NM in mammalian cells

To express in Huh-T7 cells the full-length SUD and its more stable derivative SUD-NM comprising the two macrodomains (SUD-N and SUD-M) (Tan et al., 2007), their coding sequence was placed under control of the T7 promoter in the context of the pIVEX WG vector (Roche). A complete SUD sequence was obtained from pET-Blue2-SUD (Tan et al., 2007) by digestion with NcoI and XhoI restriction enzymes. Then, the purified insert was cloned into NcoI-XhoI-treated and dephosphorylated vectors resulting in plasmids named pIVEX-SUD. A SUD-NM sequence was PCR-amplified using the proof-reading Pfu DNA polymerase, the template pQE30-Xa-SUD-NM, and the forward and reverse primers (Supplementary Table 1). The purified amplicon was treated with NcoI and SmaI and inserted into the dephosphorylated vector pIVEX WG digested with the same enzymes, resulting in plasmid pIVEX-SUD-NM.

Complementation in trans of SUD and SUD-NM and their immunological detection

Huh-T7 cells (1×10^5 cells/well) cotransfected with 0.25 μg SUD-lacking or parental SARS-CoV replicon and 1 μg pIVEX-SUD or pIVEX-SUD-NM plasmids were infected with helper vaccinia virus MVA-T7 (multiplicity of infection, moi, around 5 as previously described (Sutter et al. 1995; Kusov et al., 2002)). After one hour, the infection mixture was replaced with growth medium and incubation was continued for 48 h. To measure Renilla luciferase activity, the cells were lysed using Passive Lysis Buffer (Promega) as described above. Complementation experiments were run in triplicate and the mean values were employed for analysis. To detect viral proteins, aliquots of cell lysates were boiled with 1% sodium dodecyl sulfate (SDS) and proteins were separated by 12% denaturing polyacrylamide gel (SDS-PAGE) before transfer to PVDF membranes (Immobilon-P, Millipore). His-tagged proteins (full-length SUD or SUD-NM) were immunologically detected using either polyclonal SARS-CoV anti-Nsp3 (dilution 1:1000; Rockland, not shown) or monoclonal anti-His_4 (1:5000, Qiagen) as primary antibody. Alkaline phosphatase (AP)-conjugated anti-rabbit or anti-mouse IgG was used as a secondary antibody (1:10000, Sigma).

Docking of a G-quadruplex to SUD-NM

Atomic coordinates for a typical G-quadruplex were obtained from the Protein Data Bank (PDB; PDB code 2F8U, Dai et al., 2006). The G-quadruplex was docked into the SUD-NM structure determined previously (Tan et al., 2009) using the program AUTODOCK (Morris et al., 2009).

Acknowledgments

We thank Doris Mutschall for excellent technical assistance, Liliya Grin and Luisa Stroeh for help with the preparation and analysis of several constructs, and Dr. Jian Lei for discussion. This work was supported by the German Center for Infection Research (DZIF), the European Commission (through its projects SILVER (Contract no. 260644) and EMPERIE (Contract no. 223498)), the Ministry of Science and Innovation of Spain (BIO2010-16705), the U.S. National Institutes of Health (Grant nos. 2P01AI060699-06A1 and CRIP-HHSN266200700010C), and the Sino-German Center for the Promotion of Research, Beijing, China (GZ 236 (202/9)). The funders had no role in study design, data collection and analysis, decision to publish, or preparation of the manuscript.

Appendix A. Supporting information

Supplementary data associated with this article can be found in the online version at http://dx.doi.org/10.1016/j.virol.2015.06.016.

References

Almazán, F., Galan, C., Enjuanes, L., 2004. The nucleoprotein is required for efficient coronavirus genome replication. J. Virol. 78, 12683–12688. http://dx.doi.org/10.1128/JVI.78.22.12683-12688.2004.

Almazán, F., DeDiego, M.L., Galan, C., Escors, D., Alvarez, E., Ortego, J., Sola, I., Zuniga, S., Alonso, S., Moreno, J.L., Nogales, A., Capisco, C., Enjuanes, L., 2006. Construction of a Severe Acute Respiratory Syndrome Coronavirus infectious cDNA and a replicon to study coronavirus RNA synthesis. J. Virol. 80, 10900–-10906. http://dx.doi.org/10.1128/JVI.00385-06.

Almazán, F., Sola, I., Zuniga, S., Marquez-Jurado, S., Morales, L., Becares, M., Enjuanes, L., 2014. Coronavirus reverse genetic systems: infectious clones and replicons. Virus Res. 189, 262–270. http://dx.doi.org/10.1016/j.virusres.2014.05.026.

Anand, K., Ziebuhr, J., Wadhwani, P., Mesters, J., Hilgenfeld, R., 2003. Coronavirus main proteinase ($3CL^{pro}$) structure: basis for design of anti-SARS drugs. Science 300, 1763–1767. http://dx.doi.org/10.1126/science.1085658.

Brockway, S.M., Denison, M.R., 2005. Mutagenesis of the murine hepatitis virus nsp1-coding region identifies residues important for protein processing, viral RNA synthesis, and viral replication. Virology 340, 209–223. http://dx.doi.org/10.1016/j.virol.2005.06.035.

Dai, J., Chen, D., Jones, R.A., Hurley, L.H., Yang, D., 2006. NMR solution structure of the major G-quadruplex structure formed in the human BCL2 promoter region. Nucleic Acids Res. 34, 5133–5144. http://dx.doi.org/10.1093/nar/gkl610.

Denison, M.R., Yount, B., Brockway, S.M., Graham, R.L., Sims, A.C., Lu, X., Baric, R.S., 2004. Cleavage between replicase proteins p28 and p65 of mouse hepatitis virus is not required for virus replication. J. Virol. 78, 5957–5965. http://dx.doi.org/10.1128/JVI.78.11.5957–5965.2004.

Egloff, M.P., Malet, H., Putics, A., Heinonen, M., Dutartre, H., Frangeul, A., Gruez, A., Campanacci, V., Cambillau, C., Ziebuhr, J., Ahola, T., Canard, B., 2006. Structural and functional basis for ADP-ribose and poly(ADP-ribose) binding by viral macro domains. J. Virol. 80, 8493–8502. http://dx.doi.org/10.1128/JVI.00713-06.

Eriksson, K.K., Makia, D., Thiel, V., 2008. Generation of recombinant coronaviruses using vaccinia virus as the cloning vector and stable cell lines containing coronaviral replicon RNAs. In: Cavanagh, D. (Ed.), Methods Mol. Biol., Vol. 454; 2008, pp. 237–254. http://dx.doi.org/10.1007/978-1-59745-181-9_18.

Ge, F., Luo, Y., Liew, P.X., Hung, E., 2007. Derivation of a novel SARS-coronavirus replicon cell line and its application for anti-SARS drug screening. Virology 360, 150–158. http://dx.doi.org/10.1016/j.virol.2006.10.016.

Gillim-Ross, L., Taylor, J., Scholl, D.R., Ridenour, J., Masters, P.S., Wentworth, D.E., 2004. Discovery of novel human and animal cells infected by the Severe Acute Respiratory Syndrome Coronavirus by replication-specific multiplex Reverse Transcription-PCR. J. Clin. Microbiol. 42, 3196–3206. http://dx.doi.org/10.1128/JCM.42.7.3196-3206.2004.

Graham, R.L., Sims, A.C., Brockway, S.M., Baric, R.S., Denison, M.R., 2005. The nsp2 replicase proteins of murine hepatitis virus and Severe Acute Respiratory Syndrome Coronavirus are dispensable for viral replication. J. Virol. 79, 13399–13411. http://dx.doi.org/10.1128/JVI.79.21.13399-13411.2005.

Han, Y.-S., Chang, G.-G., Juo, C.-G., Lee, H.J., Yeh, S.-H., Hsu, J.T.-A., Chen, X., 2005. Papain-like protease 2 (PLP2) from severe acute respiratory syndrom coronavirus (SARS-CoV): expression, purification, characterization, and inhibition. Biochemistry 44, 10349–10359. http://dx.doi.org/10.1021/bi0504761.

Harcourt, B.H., Jukneliene, D., Kanjanahaluethai, A., Bechill, J., Severson, K.M., Smith, C.M., Rota, P.A., Baker, S.C., 2004. Identification of Severe Acute Respiratory Syndrome Coronavirus replicase products and characterization of papain-like protease activity. J. Virol. 78, 13600–13612. http://dx.doi.org/10.1128/JVI.78.24.13600-13612.2004.

Hattermann, K., Müller, M.A., Nitsche, A., Wendt, S., Mantke, O.D., Niedrig, M., 2005. Susceptibility of different eukaryotic cell lines to SARS-coronavirus. Arch. Virol. 150, 1023–1031. http://dx.doi.org/10.1007/s00705-004-0461-1.

Hilgenfeld, R., 2014. From SARS to MERS: crystallographic studies on coronaviral proteases enable antiviral drug design. FEBS J. 281, 4085–4096. http://dx.doi.org/10.1111/febs.12936.

Hilgenfeld, R., Peiris, M., 2013. From SARS to MERS: 10 years of research on highly pathogenic human coronaviruses. Antiviral Res. 100, 286–295. http://dx.doi.org/10.1016/j.antiviral.2013.08.015.

Johnson, M.A., Chatterjee, A., Neuman, B.W., Wüthrich, K., 2010. SARS Coronavirus-unique domain (SUD): three-domain molecular architecture in solution and RNA binding. J. Mol. Biol. 400, 724–742. http://dx.doi.org/10.1016/j.jmb.2010.05.027.

Kozak, M., 1989. The scanning model for translation: an update. J. Cell Biol. 198, 225–239.

Kusov, Y.Y., Shatirishwili, G., Klinger, M., Gauss-Müller, V., 2002. A vaccinia virus MVA-T7-mediated recovery of infectious hepatitis A virus from full-size cDNAs, both by themselves unable to complete the virus life cycle. Virus Res. 89, 75–88.

Kusov, Y., Kanda, T., Palmenberg, A., Sgro, J.-Y., Gauss-Müller, V., 2006. Silencing of hepatitis A virus infection by small interfering RNAs. J. Virol. 80, 5599–5610. http://dx.doi.org/10.1128/JVI.01773-05.

Marra, M.A., Jones, S.J.M., Astell, C.R., Holt, R.A., Brooks-Wilson, A., Butterfield, Y.S.N., Khattra, J., Asano, J.K., Barber, S.A., Chan, S.Y., Cloutier, A., Coughlin, S.M., Freeman, D., Girn, N., Griffith, O.L., Leach, S.R., Mayo, M., McDonald, H., Montgomery, S.B., Pandoh, P.K., Petrescu, A.S., Robertson, A.G., Schein, J.E., Siddiqui, A., Smailus, D.E., Stott, J.M., Yang, G.S., Plummer, F., Andonov, A., Artsob, H., Bastien, N., Bernard, K., Booth, T.F., Bowness, D., Czub, M., Drebot, M., Fernando, L., Flick, R., Garbutt, M., Gray, M., Grolla, A., Jones, S., Feldmann, H., Meyers, A., Kabani, A., Li, Y., Normand, S., Stroher, U., Tipples, G.A., Tyler, S., Vogrig, R., Ward, D., Watson, B., Brunham, R.C., Krajden, M., Petric, M., Skowronski, D.M., Upton, C., Roper, L.R., 2003. The genome sequence of the SARS-associated coronavirus. Science 300, 1399–1404. http://dx.doi.org/10.1126/science.1085953.

Memish, Z.A., Assiri, A., AlHakeem, R., Yezli, S., Almasri, M., Zumla, A., Al-Tawfiq, J.A., Drosten, C.A., Albarrak, A., Petersen, E. 2014. Middle East Respiratory Syndrome Coronavirus, MERS-CoV. Conclusions from the 2nd Scientific Advisory Board Meeting of the WHO Collaborating Center for Mass Gathering Medicine, Riyadh, Int. J. Infect. Dis. 24:51–53.10.1016/j.ijid.2014.05.001.

Morris, G.M., Huey, R., Lindstrom, W., Sanner, M.F., Belew, R.K., Goodsell, D.S., Olson, A.J., AutoDock4 and AutoDockTools4: automated docking with selective receptor flexibility, 2009. J. Comput. Chem. 30, 2785–2791. http://dx.doi.org/10.1002/jcc.21256.

Nakabayashi, H., Taketa, K., Yamane, T., Miyazaki, M., Miyano, K., Sato, J., 1984. Phenotypical stability of a human hepatoma cell line, Huh-7, in long-term culture with chemically defined medium. Gann 75, 151–158.

Neuman, B.W., Joseph, J.S., Saikatendu, K.S., Serrano, P., Chatterjee, A., Johnson, M.A., Liao, L., Joseph, P., Klaus, J.P., Yates III, J.R., Wuthrich, K., Stevens, R.C., Buchmeier, M.J., Kuhn, P., 2008. Proteomics analysis unravels the functional repertoire of coronavirus nonstructural protein 3. J. Virol. 82, 5279–5294. http://dx.doi.org/10.1128/JVI.02631-07.

Neuman, B.W., Chamberlain, P., Bowden, F., Joseph, J., 2014. Atlas of coronavirus replicase structure. Virus Res. 194, 49–66. http://dx.doi.org/10.1016/j.virusres.2013.12.004.

Pan, J., Peng, X., Gao, Y., Li, Z., Lu, X., Chen, Y., Ishaq, M., Liu, D., DeDiego, M.L., Enjuanes, L., Guo, D., 2008. Genome-wide analysis of protein–protein interaction and involvement of viral proteins in SARS-CoV replication. PLoS One 3, e3299. http://dx.doi.org/10.1371/journal.pone.0003299.

Piotrowski, Y., Hansen, G., Boomaars-van der Zanden, A.L., Snijder, E.J., Gorbalenya, A.E., Hilgenfeld, R., 2009. Crystal structures of the X-domains of a Group-1 and a Group-3 coronavirus reveal that ADP-ribose-binding may not be a conserved property. Protein Sci. 18, 6–16. http://dx.doi.org/10.1002/pro.15.

Putics, A., Fillipowicz, W., Hall, J., Gorbalenya, A.E., Ziebuhr, J., 2005. ADP-ribose-1″-monophosphatase: a conserved coronavirus enzyme that is dispensable for viral replication in tissue culture. J. Virol. 79, 12721–12731. http://dx.doi.org/10.1128/JVI.79.20.12721-12731.2005.

Rota, P.A., Oberste, M.S., Monroe, S.S., Nix, W.A., Campagnoli, R., Icenogle, J.P., Penaranda, S., Bankamp, B., Maher, K., Chen, M.H., Tong, S., Tamin, A., Lowe, L., Frace, M., DeRisi, J.L., Chen, Q., Wang, D., Erdman, D.D., Peret, T.S.T., Burns, C., Ksiazek, T.G., Pollin, P.E., Sanchez, A., Liffick, S., Holloway, B., Limor, J., McCaustland, K., Olsen-Rasmussen, M., Fouchier, R., Günther, S., Osterhaus, A.D.M.E., Drosten, C., Pallansch, M.A., Anderson, L.J., Bellini, W.J., 2003. Characterization of a novel coronavirus associated with Severe Acute Respiratory Syndrome. Science 300, 1394–1399. http://dx.doi.org/10.1126/science.1085952.

Saikatendu, K.S., Joseph, J.S., Subramanian, V., Clayton, T., Griffith, M., Moy, K., Velasquez, J., Neuman, B.W., Buchmeier, M.J., Stevens, R.C., Kuhn, P., 2005. Structural basis of Severe Acute Respiratory Syndrome Coronavirus ADP-ribose-1″-phosphate dephosphorylation by a conserved domain of nsP3. Structure 13, 1665–1675. http://dx.doi.org/10.1016/j.str.2005.07.02.022.

Serrano, P., Johnson, M.A., Chatterjee, A., Neuman, B.W., Joseph, J.S., Buchmeier, M.J., Kuhn, P., Wüthrich, K., 2009. Nuclear magnetic resonance structure of the nucleic acid-binding domain of Severe Acute Respiratory Syndrome Coronavirus nonstructural protein 3. J. Virol. 83, 12998–13008. http://dx.doi.org/10.1128/JVI.01253-09.

Shultz, D.E., Honda, M., Whetter, L.E., McKnight, K.L., Lemon, S.M., 1996. Mutations within the 5' nontranslated RNA of cell culture-adapted hepatitis A virus which enhance cap-independent translation in cultured African green monkey cells. J. Virol. 70, 1041–1049.

Snijder, E.J., Bredenbeek, P.J., Dobbe, J.C., Thiel, V., Ziebuhr, J., Poon, L.L.M., Guan, Y., Rosanov, M., Spaan, W.J.M., Gorbalenya, A.E., 2003. Unique and conserved features of genome and proteome of SARS-coronavirus, an early split-off from the coronavirus group 2 lineage. J. Mol. Biol. 331, 991–1004. http://dx.doi.org/10.1016/S0022-2836(03)00865-9.

Sutter, G., Ohlmann, V., Erfle, V., 1995. Non-replicating vaccinia virus vector efficiently expresses bacteriophage T7 RNA polymerase. FEBS Lett. 371, 9–12.

Tan, J., Kusov, Y., Mutschall, D., Tech, S., Nagarajan, K., Hilgenfeld, R., Schmidt, C.L., 2007. The "SARS-unique" domain (SUD) of SARS coronavirus is an oligo(G)-binding protein. Biochem. Biophys. Res. Commun. 364, 877–882. http://dx.doi.org/10.1016/j.bbrc.2007.10.081.

Tan, J., Vonrhein, C., Smart, O.S., Bricogne, G., Bollati, M., Kusov, Y., Hansen, G., Mesters, J.R., Schmidt, C.L., Hilgenfeld, R., 2009. The SARS-unique domain (SUD) of SARS coronavirus contains two macrodomains that bind G-quadruplexes. PLoS Pathog. 5, e1000428. http://dx.doi.org/10.1371/journal.ppat.1000428.

Tanaka, T., Kamitani, W., DeDiego, M.L., Enjuanes, L., Matsuura, Y., 2012. Severe Acute Respiratory Syndrome Coronavirus nsp1 facilitates efficient propagation in cells through a specific translational shutoff of host mRNA. J. Virol. 86, 11128–11137. http://dx.doi.org/10.1128/jvi.01700-12.

te Velthuis, A.J.W., van den Worm, S.H.E., Snijder, E.J., 2012. The SARS-coronavirus nsp7+nsp8 complex is a unique multimeric RNA polymerase capable of both *de novo* initiation and primer extension. Nucleic Acids Res. 40, 1737–1747. http://dx.doi.org/10.1093/nar/gkr893.

Wang, J.-M., Wang, L.-F., Shi, Z.-L., 2008. Construction of a non-infectious SARS coronavirus replicon for application in drug screening and analysis of viral protein function. Biochem. Biophys. Res. Commun. 374, 138–142. http://dx.doi.org/10.1016/j.bbrc.2008.06.129.

Xiao, Y., Ma, Q., Restle, T., Shang, W., Svergun, D.I., Ponnusamy, R., Sczakiel, G., Hilgenfeld, R., 2012. Non-structural proteins 7 and 8 of Feline Coronavirus form a 2:1 heterotrimer that exhibits primer-independent RNA polymerase activity. J. Virol. 86, 4444–4454. http://dx.doi.org/10.1128/JVI.06635-11.

Yang, H., Xie, H., Xue, X., Yang, K., Ma, J., Liang, W., Zhao, Q., Zhou, Z., Pei, D., Ziebuhr, J., Hilgenfeld, R., Yuen, K.Y., Wong, L., Gao, G., Chen, S., Chen, Z., Ma, D., Bartlam, M., Rao, Z., 2005. Design of wide-spectrum inhibitors targeting coronavirus main proteases. PLoS Biol. 3, 1742–1752. http://dx.doi.org/10.1371/journal.pbio.0030324.

Ziebuhr, J., Thiel, V., Gorbalenya, A.E., 2001. The autocatalytic release of a putative RNA virus transcription factor from its polyprotein precursor involves two paralogous papain-like proteases that cleave the same peptide bond. J. Biol. Chem. 276, 33220–33232. http://dx.doi.org/10.1074/jbc.M104097200.

Ziebuhr, J., Schelle, B., Karl, N., Minskaia, E., Bayer, S., Siddell, S.G., Gorbalenya, A.E., Thiel, V., 2007. Human Coronavirus 229E papain-like proteases have overlapping specificities but distinct functions in viral replication. J. Virol. 81, 3922–3932. http://dx.doi.org/10.1128/JVI.02091-06.